Journal of Sound and Vibration (2002) **256**(2), 373–381
doi:10.1006/jsvi.2001.4218, available online at http://www.idealibrary.com on IDEAL®

AN IMPLEMENTATION OF A WAVE-BASED FINITE DIFFERENCE SCHEME FOR A 3-D ACOUSTIC PROBLEM

G. Ruiz and H. J. Rice

Department of Mechanical and Manufacturing Engineering, University of Dublin, Trinity College, Dublin 2, Ireland. E-mail: ruizg@tcd.ie

(*Received* 24 *July* 2001, *and in final form* 22 *November* 2001)

1. INTRODUCTION

The Green's function based finite difference scheme proposed by Caruthers *et al.* [1] shows considerable potential as an efficient modelling tool at high frequencies. As it is formulated using fundamental solutions of the wave equation, it can maintain its accuracy at nodal spacings as low as two per wavelength. Implementation details of the technique are reported in reference [2] and the flexibility of the modelling technique is illustrated by an application to an axisymmetric radiation problem incorporating a high-speed flow [3].

In this letter, a formulation using plane wave based solutions is applied to a 3-D acoustic problem (plane wave functions were suggested in reference [1] as a viable alternative to the Green's functions and used later in references [3, 4]). The use of plane waves may, for many problems, simplify the implementation of the solution procedure and an example of an application in plate vibration by the authors is given in reference [5]. The implementation details of a number of representative boundary conditions are reported and the model is shown to give excellent results for driving frequencies from DC to those with wavelengths approaching the bi-nodal limit, although the implementation of natural radiation conditions needs more research at lower frequencies.

2. ANALYSIS

As the fundamental formulation proposed in reference [1] is quite straightforward, it is included here for completeness. Consider the computational cell shown in Figure 1. It is first assumed that the solution for the acoustic pressure $p(\mathbf{x})$ at the central position $\mathbf{x}_0$ of the harmonically driven Helmholtz equation

$$\nabla^2 p + k^2 p = 0 \tag{1}$$

may be approximated locally as a combination of m plane waves …

$$p(\mathbf{x}_0) = \sum_{j=1}^{m} \gamma_j \mathrm{e}^{-\mathrm{i}k\mathbf{d}_j \cdot \mathbf{x}_0}, \tag{2}$$

where k is the wavenumber, i is $\sqrt{-1}$ and $\mathbf{d}_j$ is the unit propagation direction vector of the jth plane wave with complex amplitude γ_j.

0022-460X/02/$35.00

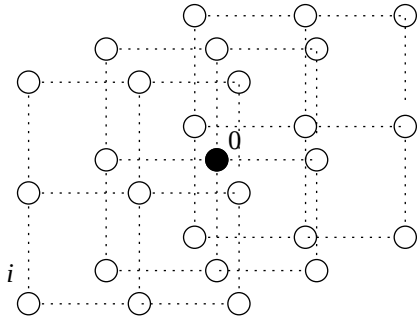

Figure 1. Fundamental computational cell.

Equation (2) may be re-expressed in matrix form as

$$p_0 = \mathbf{h}\gamma, \tag{3}$$

where $\mathbf{h}$ is an $(1 \times m)$ row vector of the plane wave functions evaluated at $\mathbf{x}_0$ and γ is a column vector of the wave strengths. If the same approximation is applied to the other nodal positions in the cell one can write

$$\mathbf{p} = \mathbf{H}\gamma, \tag{4}$$

where $\mathbf{p}$ is an $(n \times 1)$ vector of the pressures at each node i and

$$H_{ij} = \mathrm{e}^{-\mathrm{i}\mathbf{k}\mathbf{d}_j.\mathbf{x}_i}, \tag{5}$$

Equation (4) is effectively the constraint equation. A computational template may then be formed by combining equations (3) and (4) to give

$$p_0 = \mathbf{h}\mathbf{H}^+\mathbf{p}, \tag{6}$$

where superscript $+$ denotes a pseudo-inverse.

A central concept in the template proposed in equation (6) is that the number of interpolating wave functions m is greater than the number of nodes in the template less $1, \ldots, n$. Thus, the pseudo-inverse in equation (6) is not unique. If a Morse–Penrose pseudo-inverse is performed then the following properties ensue:

- All the constraints are satisfied exactly.
- The least "energetic" solution otherwise results.

Thus, boundary conditions may be implemented by augmenting the row count of the matrix $\mathbf{H}$ in equation (4) including the possibility of multiple restraints as will occur at mesh corners. Once the templates are formed, an overall sparse equation system

$$\mathbf{K}\mathbf{p} = \mathbf{f} \tag{7}$$

may be assembled with each template independently contributing a row.

3. NUMERICAL EXAMPLE

In order to demonstrate the method, a rectangular duct with an oblique ending was modelled as shown in Figure 2. The mesh was set using 27 nodes in each cell with a maximum nodal spacing of 0·05 m along the computational cell edges and 0·087 m along

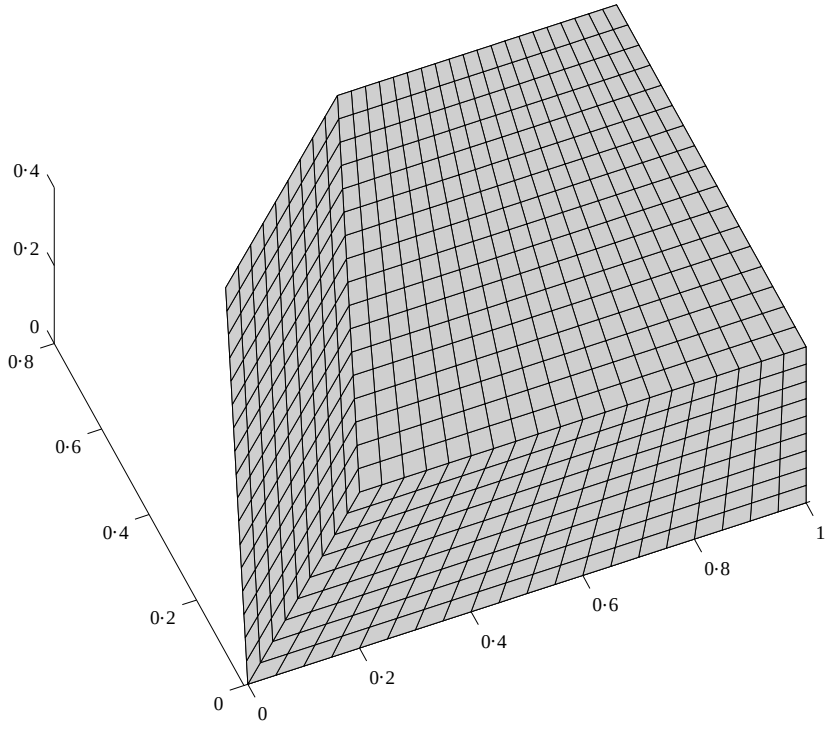

Figure 2. Test model.

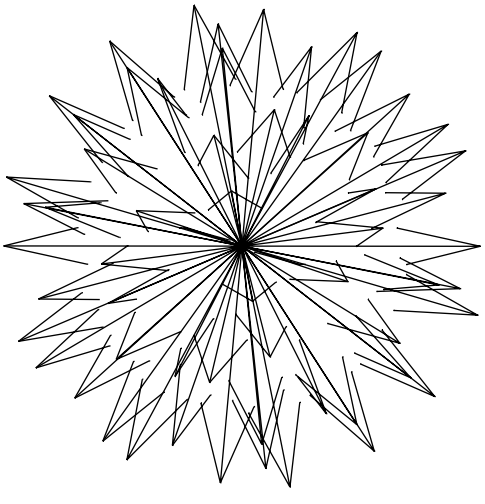

Figure 3. Wave direction system.

the diagonals. This placed the highest modelling frequency in the range 1963–3400 Hz assuming a value of 340 m/s for the sonic speed c. The cell matrices **H** and **h** in equation (6) were formulated using 60 "evenly" spaced directional waves following a buckminster fuller geodesic dome pattern (soccer ball). These are shown in Figure 3 (these directional vectors can be conveniently generated, for example, by using the © Matlab function "bucky").

Two excitation scenarios were considered, namely,

(1) *Plane wave*: In this case the duct was subject to Dirichlet condition at one end, Neumann ($\partial p/\partial \mathbf{n} = 0$) conditions were applied on the duct side and free radiation condition applied to the oblique face.
(2) *Point Source*: A Dirichlet point load was applied at one corner, Neumann conditions were applied on the adjacent faces and free radiation conditions imposed on the remaining three faces.

All of these tests were conducted over a range of driving frequencies.

3.1. BOUNDARY CONDITION IMPLEMENTATION

Owing to the flexibilty of the basic formulation, there will always be a choice of methods of imposing the boundary conditions. The solutions proposed here were chosen because they provided stable solutions for all frequencies and they were the most easily implemented from a meshing viewpoint.

3.1.1. *Dirichlet*

These were implemented by simply directly constraining the appropriate row in the assembled matrix equation (7).

3.1.2. *Neumann*

At each face/edge/corner it was found to be more convenient to use half/quarter/eight portions of the original computational cell. Thus, at an edge for example as shown in Figure 4, an $\mathbf{H}$ matrix of dimension $(17 \times m)$ is formed. At each node on the surface ($\mathbf{x}_i^b$) the boundary condition

$$\frac{\partial p}{\partial \mathbf{n}_i}(\mathbf{x}_i^b) = q_i \tag{8}$$

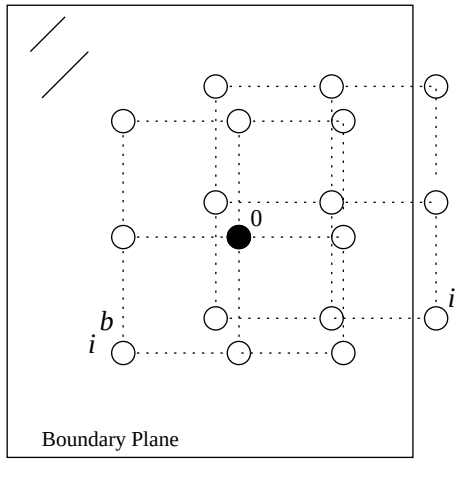

Figure 4. Edge computational cell.

is applied to augment the constraint equation (4) to

$$\begin{pmatrix} \mathbf{p} \\ q_i \\ . \\ . \end{pmatrix} = \begin{pmatrix} \mathbf{H} \\ \dfrac{\partial}{\partial \mathbf{n}_i}\ \mathbf{h}(\mathbf{x}_i^b) \\ . \\ . \end{pmatrix} \gamma, \tag{9}$$

where $\mathbf{n}_i$ is the direction of the outward normal at the boundary point $\mathbf{x}_i^b$. The augmented $\mathbf{H}_{aug}$ matrix should now have dimension $(17 + 9) \times m$. A pseudo-inverse may now be performed and the resulting matrix left–right partitioned to yield the template equation which now includes a forcing term …

$$p_0 = \mathbf{h}(\mathbf{H}_{aug}^{+})_L \mathbf{p} + \mathbf{h}(\mathbf{H}_{aug}^{+})_R \mathbf{q}. \tag{10}$$

Here $\mathbf{q}$ is a (9×1) column vector of the forcing nodal loads q_i. For a perfectly reflecting surface, q is set to zero. Note that this must always be explicitly specified using a modified template 13 as perfect reflection is not a "natural" boundary condition as would be in the case of say in a common finite element analysis.

3.1.3. *Radiation*

Two approaches to modelling this condition are possible Item

- Use of "ρc" type normal impedance approximation.
- Exclusive use of outward propagating waves in the fundamental computational template formulation.

The first technique, though an approximation which is strictly valid only for plane waves propagating normal to the surface, has several features to recommend it.

(1) Meshing can usually be formulated to ensure that the farfield solution approximately propagates normal to the radiation boundary. Thus, the degree of error incurred will be slight.
(2) It returns a robust equation system which appears to generate stable solutions over the entire frequency range.
(3) Its implementation is straightforward and is as follows. To implement the boundary condition

$$\frac{\partial p}{\partial \mathbf{n}}(\mathbf{x}_i^b) = -\,\mathrm{i}\,\frac{\rho\omega}{Z}\,p(\mathbf{x}_i^b) \tag{11}$$

at a face where ω is the frequency, ρ is the fluid density and the surface normal impedance is $Z = \rho c$, entails augmenting relationship (9) for the half template to

$$\begin{pmatrix} \mathbf{p} \\ 0 \\ . \\ . \end{pmatrix} = \begin{pmatrix} \mathbf{H} \\ \dfrac{\partial}{\partial \mathbf{n}_i}\ \mathbf{h}(\mathbf{x}_i^b) + \mathrm{i}\ \dfrac{\rho\omega}{Z}\ \mathbf{h}(\mathbf{x}_i^b) \\ . \\ . \end{pmatrix} \gamma. \tag{12}$$

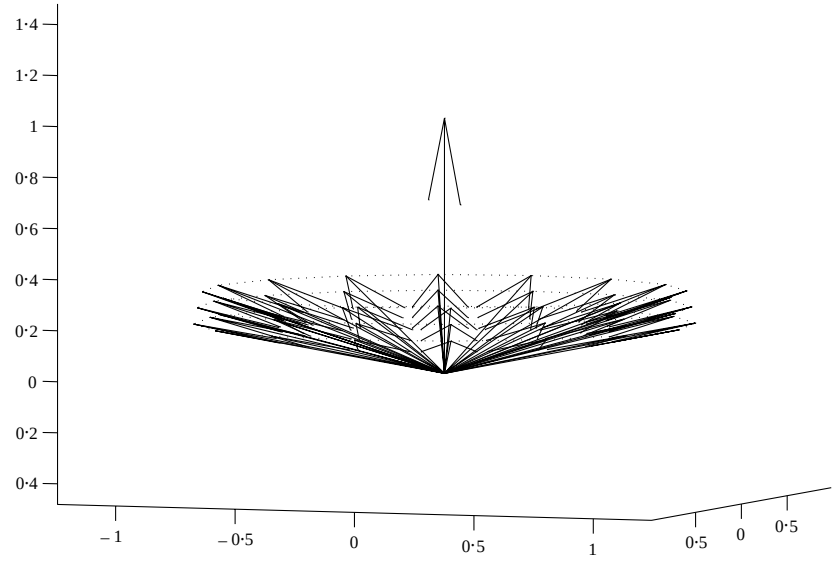

Figure 5. Optimized radiation vector set.

After inversion and partitioning, template (13) then reduces to

$$p_0 = \mathbf{h}(\mathbf{H}^{+}_{aug})_L \mathbf{p}. \tag{13}$$

The second method which follows the concept of establishing a "natural" radiation condition for the method as primarily advanced in reference [1] is that appropriate partial templates should be used in conjunction with a special $\mathbf{H}_{rad}$ wave-function matrix. This is a reduction of the original matrix which includes only *outward* propagating directions at a particular boundary. The template is then given simply by

$$p_0 = \mathbf{h}\mathbf{H}^{+}_{rad}\mathbf{p}. \tag{14}$$

In principle, this approach is error free, however, the authors have found system conditioning problems emerging when attempting to use this approach over a wide range of frequencies. In this letter, an alternative compromise approach is described which restored solution robustness without loss of accuracy. An $\mathbf{H}_{rad}$ function matrix was generated using 49 directions which fell within an optimized 75° cone normal to the boundary as shown in Figure 5. The precise formulation of this optimization is still under investigation. Thus, if a mesh is established which ensures that outward waves are propagating at angles within 37·5° of the normal, then no error results. This condition is easily met if the mesh is convex and reasonably clear of nearfield activity.

3.1.4. *Combination/Corners*

The precedent Neumann and Radiation boundary condition methods can be readily combined should more than one restraint need to be imposed at the boundary points.

If a ρc approach is used for the radiation boundary condition, then equations (9) and (12) are used in conjuntion to augment $\mathbf{H}$ according to the normal directions. For the natural radiation boundary approach, first an $\mathbf{H}_{rad}$ is constructed from the correspondent outward directions *only* and then augmented using relationship (9).

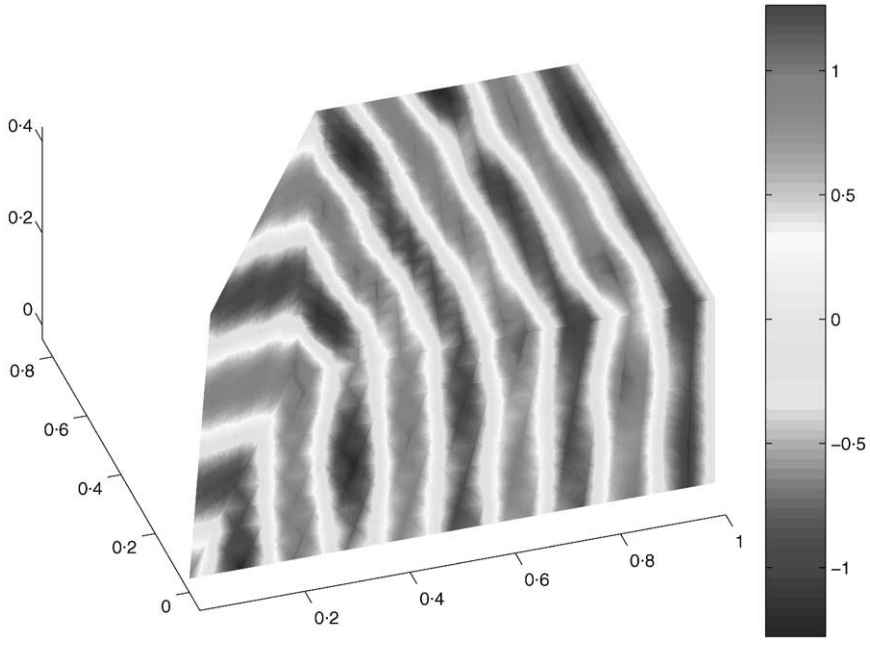

Figure 6. Plane wave solution, ρc approach. Freq. = 1600 Hz. Imaginary pressure value.

3.2. RESULTS

3.2.1. *Plane wave*

The results obtained with a "ρc" approach in the oblique radiating face, show the distortion resulting in the pressure distribution when the propagating wave is not normal to the boundary. The violation of the normal propagation requirement clearly results in waves being reflected back from the oblique face: Figure 6.

The compromise "natural" boundary radiating approach, gives effectively an error-free solution with an accuracy of up to 4.25 and 2.45 points per wavelength for the minimun and maximun cell distance, respectively, Figure 7. It should be noted that no distortion is observed at the corners of the free radiating face, where a Neumann-radiation combination was used.

3.2.2. *Point source*

The natural radiation method shows the same accuracy for modelling a free spherical radiating wave, Figure 8. A loss of stability was observed, however, for frequencies below 400 Hz. The increment in the condition number of **K** (equation (7)) was found to be related to the outward directions in the axis parallel faces.

At low frequencies, on the other hand, the "ρc" approach will give an accurate solution. However, it was found that by slightly perturbing the wave some of the wave speeds used in the selection of allowed outward propagation direction "cone" restored solution stability to the natural radiation formulation.

4. CONCLUSIONS

(1) The general approach is shown to be robust, practical to implement for general 3-D problems.

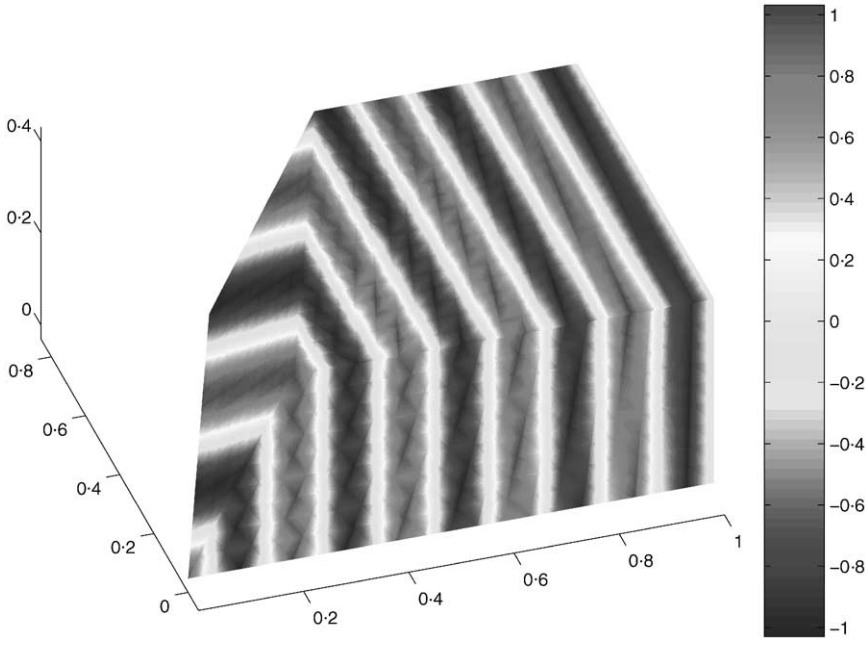

Figure 7. Plane wave solution, natural approach. Freq. = 1600 Hz. Imaginary pressure value.

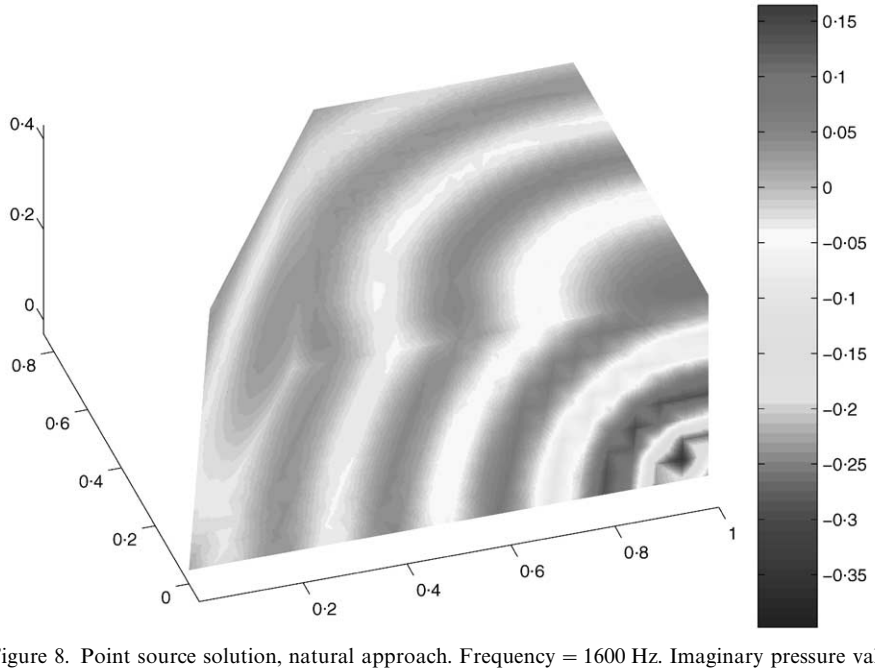

Figure 8. Point source solution, natural approach. Frequency = 1600 Hz. Imaginary pressure value.

(2) Meshing restraints and difficulties associated with the modelling of corners are absent.
(3) A natural radiation boundary condition is viable.

(4) An objective assessment of its computational advantage has yet to be performed. As is clear, a low nodal density is viable with a similar system matrix bandwidth to a quadratic finite element formulation. The formulation is however, not symmetric, but as each nodal degree of freedom generates rows of the system matrix independently, there may be computional advantages evident in the evolution of iterative-type solutions for large problems. Assembly time is moderate even if the computational cells are not identical and will for large problems be dominated by the solution of the system equation (7).

ACKNOWLEDGMENT

The support of the Trinity College Centre for High Performance Computing is gratefully acknowledged.

REFERENCES

1. J. E. CARUTHERS, J. C. FRENCH and G. RAVINPRAKSH 1995 *Journal of Sound and Vibration* **187**, 553–568. Green's function discretization for numerical solution of the Helmholtz equation. doi: 10.1006/jsvi.1995.0544
2. J. E. CARUTHERS, J. C. FRENCH and G. RAVINPRAKSH 1995 *CEAS/AIAA*-95-117. Recent developments concerning a new discretization method for the Helmholtz equation.
3. J. E. CARUTHERS, R. C. ENGELS and G. RAVINPRAKSH 1996 *AIAA/CEAS*-96-1684. A wave expansion method for discrete frequency acoustics within inhomogeneous flows.
4. J. E. CARUTHERS, J. S. STEINHOFF and R. C. ENGELS 1999 *Journal of Computatinal Acoustics* **7**, 245–252. An optimal finite difference for a class of linear PDE's with applications to the Helmholtz equation.
5. H. J. RICE and G. RUIZ 2000 *ISMA*25, 1477–1482. A finite difference analysis of plate vibration using a wave expansion technique.